ChemPubSoc Europe

DOI: 10.1002/open.201800100

Open Access ChemistryOPEN Full Papers

Spectrochemical Properties and Solvatochromism of Tetradentate Schiff Base Complex with Nickel: Calculations and Experiments

Agnieszka Gonciarz,*[a] Marian Żuber,[b] and Jerzy Zwoździak[c]

The nickel(II) complex with a tetradentate Schiff base ligand obtained by condensation of 1,3-propanediamine with salicylaldehyde (H_2salpn) was studied in a variety of solvents at room temperature. The product, that is, the *N*′,*N*′′-propylenebis(salicylaldiminato)nickel(II) ([Ni(salpn)]) complex, is brown in color in the solid state. The properties of the ligand and complex were characterized by elemental analysis, solubility in common solvents, molar conductivities, and ultraviolet (UV) and visible (Vis) spectroscopy. The [Ni(salpn)] complex is easily soluble in common solvents such as chloroform, methanol, ethanol, dimethyl formamide, dimethyl sulfoxide, acetonitrile, dioxane, acetone, 2-propanol, and toluene—a necessary condition for observing solvatochromism. The molar conductivity values, equal to 0.0 $S\,mol^{-1}\,cm^2$ in these solvents, point to a typical non-electrolyte behavior for this complex. Spectroscopic measurements were used to confirm the square-planar geometry of the species in solution and to determine the coordination properties of the donor atoms and their bonding abilities (CFM/AOM parameters), as well as trichromaticity coordinate calculations. The results obtained show that the interactions of the metal with the donors depend on the polarity of the solvent.

1. Introduction

Schiff bases, named after Hugo Schiff, belong to a class of compounds that contain an imine or azomethine group (–RC=N–). They are usually formed by the condensation of a primary amine with an active carbonyl compound. Interest in the chemistry of Schiff bases and their metal complexes has increased in recent decades, because of the wide applications of these compounds in various fields. Schiff bases have been shown to exhibit a broad range of biological activities, including antifungal,[1] anticancer,[2] antibacterial,[3] antimalarial,[3] anti-inflammatory,[4] antiviral,[5] and antipyretic and herbicidal[6] properties. However, the chelation of Schiff bases with transition-metal ions was reported to improve the biological potentials of Schiff bases; hence, metal complexes of various Schiff bases are renowned as antibacterial, antifungal, anticancer, and antioxidant agents. Alias et al.[7] showed that a nickel(II) complex with a Schiff base exhibited high inhibition activity against the two bacteria used in their study; this activity was comparable to that of standard drugs. Also, Adb El-Halim[8] studied Schiff base ligands derived from pyridine-2,6-dicarboxaldehyde and their nickel(II) complexes for biological activity against bacterial species and fungi. They showed that the antibacterial and antifungal activities of the metal complexes were higher than those of the parent Schiff base ligands against one or more bacterial or fungi species. Schiff bases are also some of the most widely used organic compounds. They are used as pigments and dyes, catalysts, intermediates in organic synthesis, and polymer stabilizers.[9] They have widely been investigated as liquid-crystalline materials and can be used, for example, in optoelectronics.[10] Also, Schiff base complexes with transition metals have been studied for their interesting and important properties. Over the past few years, there have been many reports on their application in homogeneous and heterogeneous catalysis, their use as catalysts for oxidation and epoxidation reactions, and their use as synthetic oxygen carriers. They were previously reported to be useful models for bioinorganic processes.[11,12]

This paper is a continuation of our studies on the coordination chemistry of tetradentate Schiff base.[13] These Schiff bases are interesting, because they can form complexes with nickel(II) ions with different geometries. We focused on interpreting the electronic spectra of the square-planar, diamagnetic nickel(II) complex with a Schiff base ligand derived from sali-

[a] *Dr. A. Gonciarz*
Department for Security Studies
The General Tadeusz Kosciuszko Military University of Land Forces
Czajkowskiego Str. 109, 51–147 Wroclaw (Poland)
E-mail: agnieszka.gonciarz@awl.edu.pl

[b] *Prof. Dr. M. Żuber*
Department for Security Studies
The General Tadeusz Kosciuszko Military University of Land Forces
Czajkowskiego Str. 109, 51–147 Wroclaw (Poland)

[c] *Prof. Dr. J. Zwoździak*
Department for Security Studies
The General Tadeusz Kosciuszko Military University of Land Forces
Czajkowskiego Str. 109, 51–147 Wroclaw (Poland)

The ORCID identification number(s) for the author(s) of this article can be found under: https://doi.org/10.1002/open.201800100.

© 2018 The Authors. Published by Wiley-VCH Verlag GmbH & Co. KGaA. This is an open access article under the terms of the Creative Commons Attribution-NonCommercial License, which permits use, distribution and reproduction in any medium, provided the original work is properly cited and is not used for commercial purposes.

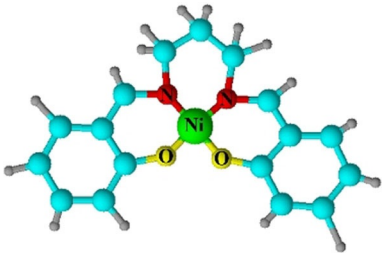

Scheme 1. Simulation structure of the nickel(II) complex with 1,3-bis(salicylideneimino)propane. The optimization was performed by using the ChemSketch program.

cylaldehyde and 1,3-propanediamine (Scheme 1) in different solvents.

The main aim of this study was to determine the structure of the complex in solution and to explain the solvent effects. This was considered from two viewpoints: 1) solvation effects on the structure of the complex; 2) solvatochromic effects on the UV/Vis spectra.

Coordination and solvent effects may lead to significant changes in the d–d transitions (square planar↔octahedral)[14] and to a large change in the ligand-field parameters of the complexes in solution. We extended this paper to include results on chromaticity because solvents can change the color of the solution. This effect can be difficult to observe visually, and changes in colors in dilute solutions are particularly subtle. For this reason, for precise characterization of the color we used tristimulus colorimetry.

2. Results and Discussion

The tetradentate Schiff base and its nickel(II) complex were synthesized and characterized by elemental analysis, molar conductivities, IR spectroscopy, ultraviolet (UV) spectroscopy, and visible (Vis) spectroscopy. The elemental analysis results of the Schiff base ligand and its nickel(II) complex agree well with the expected composition of the studied complex and support the fact that the mole ratio of Schiff base to the metal complex is 1:1, as shown in Scheme 1.

2.1. IR Spectra of the Ligand and Nickel(II) Complex

The metal–ligand bond was confirmed by comparing the IR spectra of the Schiff base ligand and the nickel(II) complex. The IR spectrum of the nickel(II) complex shows the typical bands of the Schiff base, with the strong band at $\tilde{\nu}=$ 1611 cm^{-1} assigned to ν(C=N). We can see that the ν(C=N) band in the complex is shifted by $\Delta\tilde{\nu}=25$ cm^{-1} to the lower energy region in the corresponding free ligand ($\tilde{\nu}=$ 1636 cm^{-1}). The shift of the spectrum of the complex to lower energy suggests coordination of the azomethine nitrogen atom to the metal ion. The high-intensity band at the lower energy of 1279 cm^{-1} for the Schiff base is due to the phenolic C–O stretching frequency. In the complex, the C–O stretching vibration appears at a slightly lower frequency, $\tilde{\nu}=1228$ cm^{-1}, which confirms coordination through the phenolic oxygen atom. According to many authors,[11,15,16] characteristic absorption bands for nickel(II)–N and nickel(II)–O appear in the spectral regions of $\tilde{\nu}=650$ to 850 cm^{-1} and $\tilde{\nu}=400$ to 600 cm^{-1}, respectively. New bands, in the studied complex, are observed at $\tilde{\nu}=745$ and 460 cm^{-1}, and they can be assigned to ν(Ni-N) and ν(Ni-O), respectively; they are absent in the spectrum of the free ligand. These results show that the Schiff base ligand with the N_2O_2-type donor atom set behaves in a tetradentate manner binding to the metal ion through the phenolic oxygen atoms and the azomethine nitrogen atoms.

2.2. UV Spectra of the Ligand and Ni^{II} Complex

Salicylaldimines have widely been studied spectroscopically.[17,18] The electronic spectra of 1,3-bis(salicylideneimino)propane (H_2salpn) in DMF, EtOH, and hexane solutions were previously reported.[15,19] In our study, we expanded the amount of solvents to nine, methanol (MeOH), ethanol (EtOH), 2-propanol (*i*PrOH), dimethyl sulfoxide (DMSO), acetonitrile (MeCN), dimethylformamide (DMF), chloroform ($CHCl_3$), dioxane (DX), and toluene (MBz), to investigate the influence of solvent polarity on the spectroscopic properties of the Ni–Schiff base complex. Figure 1 presents the electronic spectra of H_2salpn in a variety

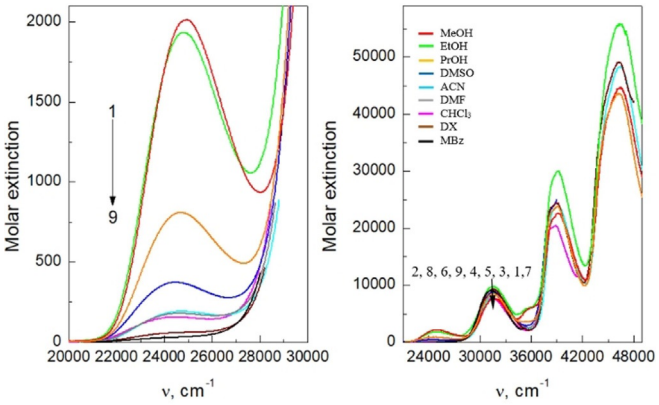

Figure 1. Electronic absorption spectra of H_2salpn in solution in the UV region. 1: MeOH, 2: EtOH, 3: *i*PrOH, 4: DMSO, 5: MeCN, 6: DMF, 7: $CHCl_3$, 8: DX, 9: MBz.

of solvents in the UV region. All nine spectra show similar shapes and exhibit band maxima at about $\nu=24600$, 31500, 39000, and 46000 cm^{-1}, depending on the solvent applied. If the range of the electronic spectrum was shorter, for example, in DMF and DMSO, the spectrum fewer bands were observed, because there is not transmittance above $\nu=38000$ cm^{-1}. Bosnich attributed the first band to a $n\rightarrow\pi^*$ transition involving promotion of one of the lone pair of electrons of the nitrogen atom to the antibonding π orbital associated with the azomethine group, whereas the band at $\nu=31000$ cm^{-1} corresponds to a $\pi\rightarrow\pi^*$ transition.[20] For the maximum at $\nu=24600$ cm^{-1}, a hypochromic effect can be observed (see Table 1).

In our study, we compared the hypochromic effect with the solvent parameters. It was observed that the intensity of the band decreased upon decreasing the acceptor number (AN),

© 2018 The Authors. Published by Wiley-VCH Verlag GmbH & Co. KGaA, Weinheim

Table 1. Correlation between the intensity of the absorption maximum at $\nu = 24\,600\ cm^{-1}$ and selected solvent parameters for [Ni(salpn)] in the studied solvents.[a]

Solvent	ε [$M^{-1}cm^{-1}$]	AN	Z	E_T^N
MeOH	2010	41.5	83.6	0.762
EtOH	1960	37.1	79.6	0.654
*i*PrOH	790	33.5	76.3	0.546
DMSO	360	19.3	70.2	0.444
MeCN	190	18.9	71.3	0.460
DMF	180	16.0	68.4	0.386
$CHCl_3$	150	23.1	63.2	0.259
DX	60	10.8	64.5	0.164
MBz	30	6.8	54.0	–

[a] ε: molar extinction coefficient, AN: acceptor number, Z: Kosower parameter, E_T^N: Dimroth–Reichardt parameter.

the Kosower parameter (Z), and the Dimroth–Reichards parameter (E_T^N).

The spectra of the ligand were resolved into Gaussian components in the $\nu = 20\,000$–$50\,000\ cm^{-1}$ region. Kurzak et al.[21] synthesized the Schiff base derived from salicylaldehyde and ethylenediamine (H_2salen) and quantitatively interpreted the electronic spectra in MeOH, DMSO, DMF, and $CHCl_3$ solution in the UV region. The electronic spectra of H_2salen and H_2salpn are very similar. Therefore, in our studies the experimental curve of the Schiff base (H_2salpn) was resolved into ten component bands on the basis of the literature data mentioned above (for the UV region). These bands were used to analyze the spectra of the complex in the UV region. Figure 2a shows the electronic spectrum of the H_2salpn ligand in EtOH solution along with the Gaussian components.

Figure 3 shows the electronic spectra of [Ni(salpn)] in different solvents in the UV region. All the spectra show maxima at about $\nu = 24\,500$, 29 000, 38 000, and $41\,000\ cm^{-1}$. Usually, the absorption bands occurring at around $\nu = 24\,500$ and $37\,500\ cm^{-1}$ can be attributed to charge-transfer (CT) transition.[11,15,16] Therefore, on the basis of our previous studies and the literature, we assigned the band at roughly $\nu = 24\,500\ cm^{-1}$ to the metal-to-ligand charge-transfer (MLCT) transition ($Ni^{2+} \rightarrow O_{aldehyde}$) and the high-energy band at around $\nu = 38\,000\ cm^{-1}$ to the MLCT transition ($Ni^{2+} \rightarrow N_{imine}$). The spectra were resolved into Gaussian components. Their number was assumed by analysis of the spectra of H_2salpn and the additional CT and d–d bands predicted for the complex. Figure 2b shows the UV experimental absorption spectra of [Ni(salpn)] with Gaussian-type curves in EtOH solution, and Table 2 presents a comparison of the transition energies and intensities of the component bands resulting from Gaussian analysis for the ligand and the [Ni(salpn)] complex in EtOH solution, as well as the assignment of the bands.

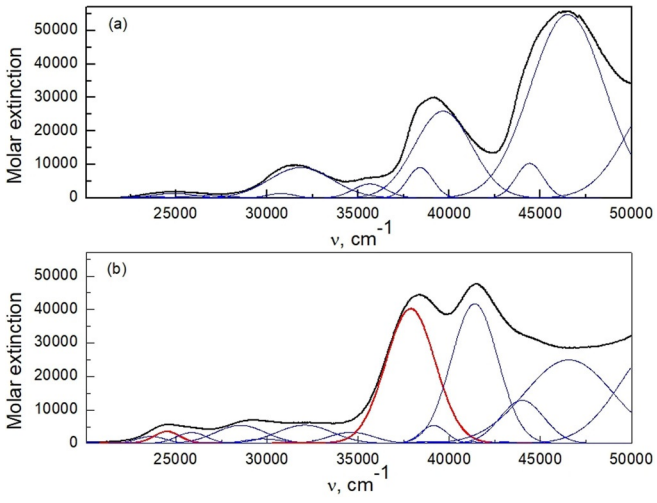

Figure 2. Experimental electronic spectra (——) along with Gaussian components (——: IM transition, (——: CT transition) in the UV region of a) H_2salpn and b) [Ni(salpn)] in EtOH solution.

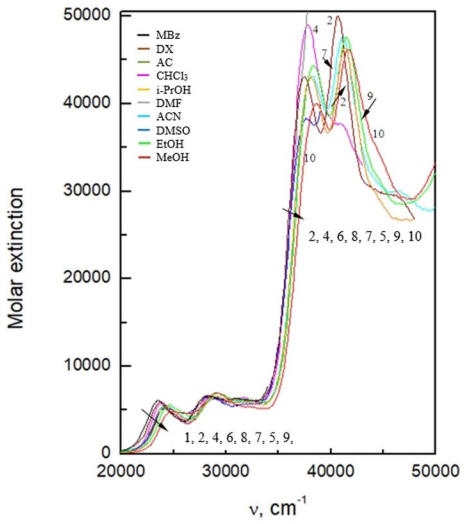

Figure 3. Electronic absorption spectra of [Ni(salpn)] in solution in the UV region. 1: MBz, 2: DX, 3: AC, 4: $CHCl_3$, 5: *i*PrOH, 6: DMF, 7: MeCN, 8: DMSO, 9: EtOH, 10: MeOH.

2.3. Visible Spectra and Ligand-Field Analysis

In this part of our study, we focused on interpretation of the electronic spectra of the [Ni(salpn)] complex in various solvents. The X-ray data for this complex are known.[22] The nickel atom is in a regular square-planar environment and is coordinated by two oxygen donors and two imine nitrogen donors. The Ni–N and Ni–O distances are 1.901 and 1.845 Å, respectively. As seen in the complex, the Ni–N and Ni–O bond lengths are very close (within experimental error). The *cis* configuration is imposed by the geometry of the tetradentate NOON ligand in this complex (C_{2v} symmetry point group). It is generally known that straight transferal of the geometry between the X-ray structure (crystal lattice) and the structure in solution is not legitimate. In solution, the following processes can be expected: 1) partial or complete dissociation causing ionization of the solute; 2) interaction of a solute with the solvent molecules (solvation); solvation of the transition-metal complex can also occur by formation of coordination bonds (as in $[M(solvent)_n]^{m+}$), that is, solvent coordination or substitution of the ligands. Some physicochemical measurements for

© 2018 The Authors. Published by Wiley-VCH Verlag GmbH & Co. KGaA, Weinheim

Table 2. The intensities (ε_{max}) and positions (ν_{max}) of the component bands resulting from Gaussian analysis for H_2salpn and [Ni(salpn)] in EtOH solution in the UV region.

No.	ε_{max} [10^{-3} м$^{-1}$ cm^{-1}] H_2salpn	ν_{max} [10^{-3} cm^{-1}]	ε_{max} [10^{-3} м$^{-1}$ cm^{-1}] [Ni(salpn)]	ν_{max} [10^{-3} cm^{-1}]	Assignment[a]
1	0.57	23.56	2.08	23.63	IM
2	–	–	3.25	24.46	CT
3	1.53	24.85	3.40	25.78	IM
4	0.8	26.83	5.41	28.53	IM
5	1.48	30.76	1.37	29.77	IM
6	9.13	31.85	5.48	32.06	IM
7	4.16	35.63	3.36	34.62	IM
8	–	–	0.24	37.74	d–d
9	–	–	40.22	37.89	CT
10	–	–	0.50	38.50	d–d
11	–	–	0.51	39.13	d–d
12	9.19	38.39	5.38	39.14	IM
13	–	–	0.14	40.23	d–d
14	–	–	0.46	41.33	d–d
15	25.95	39.65	41.73	41.39	IM
16	–	–	0.22	42.77	d–d
17	–	–	0.50	43.00	d–d
18	10.43	44.39	12.90	43.99	IM
19	55.04	46.49	24.99	46.56	IM
20	–	–	0.07	48.65	d–d

[a] IM: intramolecular, CT: charge transfer.

the solution can exclude either process or one of them. In our investigations, the molar conductivity and absorption electronic spectra were used to postulate the geometry of the species in solution.

The conductance values of [Ni(salpn)] in solutions of $CHCl_3$, DX, MBz, acetone (AC), MeCN, DMF, DMSO, EtOH, MeOH, and *i*PrOH are 0.0, 0.1, 0.0, 0.0, 0.2, 0.0, 0.0, 0.0, 0.8, and 0.0 S mol^{-1} cm^2, respectively. Very low values of the molar conductivity suggest non-electrolyte properties of [Ni(salpn)] in all solutions and excludes dissociation of the complex. Evidently, if ionic species exist in solution, they are electrically conductive. In a neutral metal/ligand = 1:1 type complex, dissociation without coordination of the solvent is impossible.

As mentioned above, the second effect expected in solution is solvation. Because of this process, a six-coordinate nickel(II) complex (octahedral or pseudo-octahedral, paramagnetic) species can arise. If the solvent molecules are coordinated as a ligand, then four-coordinate solvates are unlikely. Furthermore, the electronic absorption spectra exclude the existence of the six-coordinate form in solution. This significantly differs from that observed for four-coordinate nickel(II) complexes (square planar, diamagnetic). Namely, the former exhibit two low-energy bands with low-intensity maxima at around ν = 8000–9000 and 15 000–16 000 cm^{-1} (molar extinction coefficients are from a few dozen to over a dozen or so). In contrast, the electronic spectra of diamagnetic, square-planar, four-coordinate complexes display only one band with a high-intensity maximum at ν = 16 000–19 000 cm^{-1}[23–26] (molar extinction coefficients are from several dozen to a few hundred dozen or so).

Figure 4 shows the experimental electronic spectra of [Ni(salpn)] in all studied solvents in the visible region. A hypochromic effect is visible for the observed bands as follows: MBz > DX > AC ≈ $CHCl_3$ > *i*PrOH > DMF > MeCN > DMSO > EtOH > MeOH. This dependence cannot be connected with any property of the solvents. All spectra are similar in shape and exhibit only one maximum at about ν = 17 000 cm^{-1} and a shoulder at about ν = 18 500 cm^{-1}. These are characteristic of square-planar diamagnetic nickel(II) chelates, and correspond to the d–d transitions. Thus, the electronic absorption spectra exclude a six-coordinate form in all solutions. Also, in our stud-

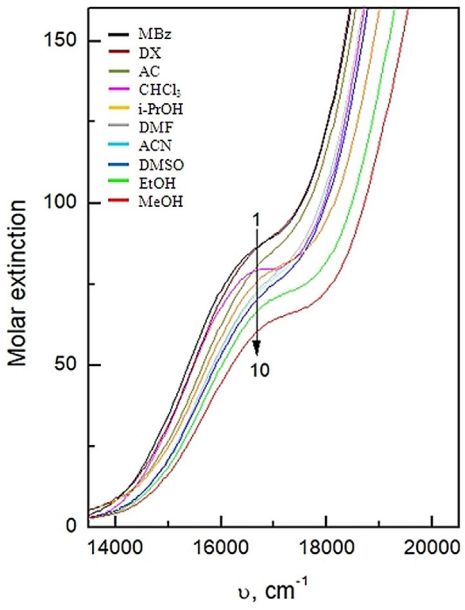

Figure 4. Electronic absorption spectra of the [Ni(salpn)] in solution in the visible region. 1: MBz, 2: DX, 3: AC, 4: $CHCl_3$, 5: *i*PrOH, 6: DMF, 7: MeCN, 8: DMSO, 9: EtOH, 10: MeOH.

© 2018 The Authors. Published by Wiley-VCH Verlag GmbH & Co. KGaA, Weinheim

ies, zeroed absorption in the near-IR region was observed (reflectance spectra).

The basis for quantitative interpretation of a spectrum is to determine the symmetry of a molecule. The H_2salpn ligand has two different donor atoms. The oxygen atom from the hydroxy group has different π interactions than the nitrogen atom from the amine group. Oxygen-donor atoms exhibit different π interactions, that is, $\pi\parallel$ and $\pi\perp$ to the salicylic ring, whereas nitrogen-donor atoms present only $\pi\perp$ interactions. If the differences between the oxygen and nitrogen donors are taken into account, the symmetry group of [Ni(salpn)] is significantly lower, that is, C_{2v}. If all the interactions between the nickel(II) ion and the donor atoms are allowed, then seven angular overlap model (AOM) parameters should be calculated [e_σ (O), $e_{\pi\parallel}$ (O), $e_{\pi\perp}$ (O), e_σ (N), $e_{\pi\perp}$ (N), *B*, and *C*]. Because of the overparameterization problem (calculating more parameters than variables), in our opinion the assumed geometry (D_{4h} as effective symmetry) is acceptable for the studied complex. For this reason, the AOM parameters were calculated as averages for the nitrogen- and oxygen-donor atoms. The ligand-bonding abilities are characterized by an anisotropic π interaction, that is, $e_{\pi\parallel}$ and $e_{\pi\perp}$ parameters are taken into account. Finally, we considered five parameters, that is, three AOM (e_σ, $e_{\pi\parallel}$, $e_{\pi\perp}$) and two Racah interelectron repulsion parameters (*B*, *C*; $C/B \approx 4$).

Figure 5 shows the experimental spectra of the nickel(II) complex in the visible region in nonpolar solutions with Gaussian lines curves, and Figures 6 and 7 show similar spectra in polar solvents. The spectra were resolved into six component

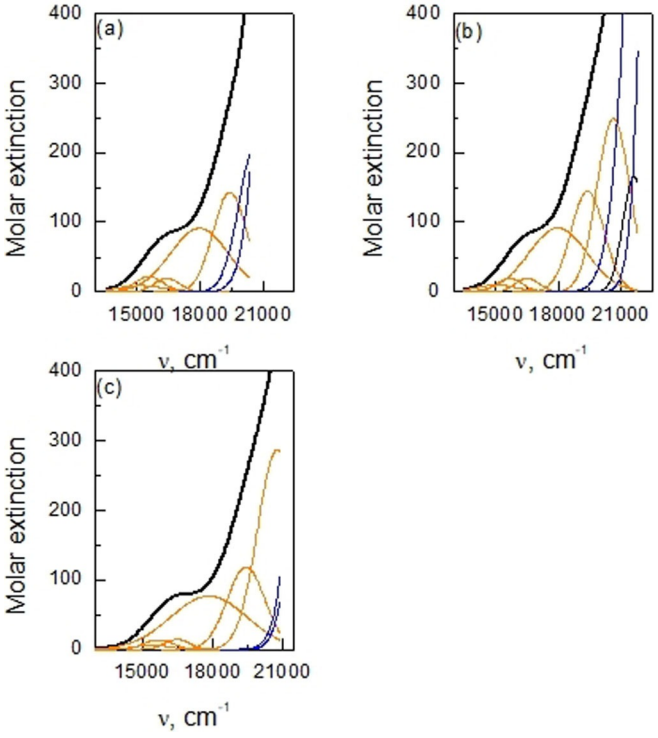

Figure 5. Electronic spectra and Gaussian line shapes (——: d–d transition, ——: CT or IM transition) of [Ni(salpn)] at room temperature in the visible region in nonpolar solvents: a) MBz, b) DX, and c) $CHCl_3$.

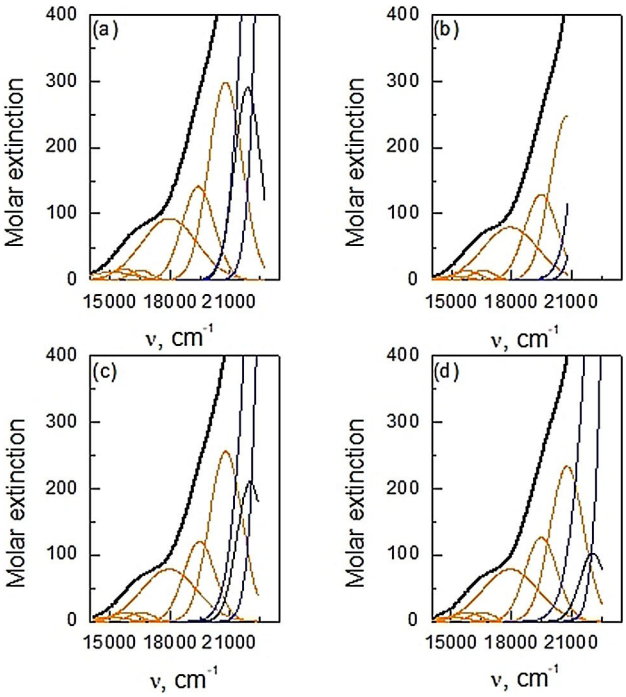

Figure 6. Electronic spectra and Gaussian line shapes (——: d–d transition, ——: CT or IM transition) of [Ni(salpn)] at room temperature in the visible region in polar solvents: a) AC, b) DMF, c) DMSO, and d) MeCN.

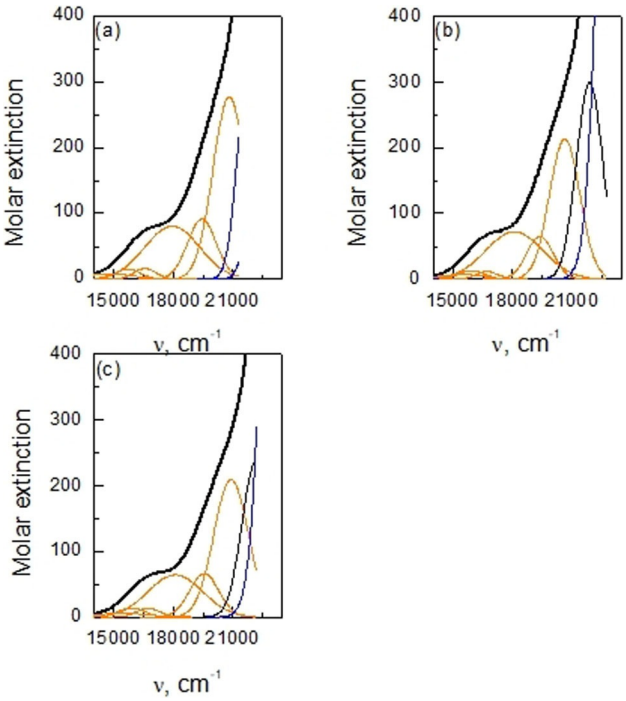

Figure 7. Electronic spectra and Gaussian line shapes (——: d–d transition, ——: CT or IM transition) of [Ni(salpn)] at room temperature in the visible region in polar solvents: a) *i*PrOH, b) EtOH, and c) MeOH.

bands. In general, the unique procedure, which starts with Gaussian analysis, by assigning the bands and calculation of chemically useful parameters, is based on two assumptions: 1) the symmetry of a compound is known; 2) the theoretical

© 2018 The Authors. Published by Wiley-VCH Verlag GmbH & Co. KGaA, Weinheim

model (e.g. ligand-field model for the complex) is adequate to calculate the spectral parameters. Our calculations take into account all d–d transitions that are given by ligand-field theory, even those that are strongly overlapped. In the visible region, all bands may be attributed to d–d transitions, except one band at approximately $v = 21\,900\ cm^{-1}$, which is not predicted by ligand-field theory, that is, this band is not a d–d transition.

The transition energies, their assignments, values of the crystal field model (CFM) and AOM parameters, and the root-mean-square error (RMS) for polar and nonpolar solvents are summarized in Tables 3 and 4. The best fit with the experimental data was obtained for these results.

The title nickel(II) complex with a Schiff base ligand derived from salicylaldehyde and 1,3-propanediamine may be diamagnetic according to some authors[27] or may be paramagnetic according to others.[19] Csaszar and Balog synthesized a paramagnetic (six-coordinate) form of this complex with the magnetic moment of the solid state equal to 3.28 BM.[19] The Racah *B* parameter calculated by them from the reflectance spectra of this chelate crystallized from pyridine was 992 cm^{-1}. Singh et al.[28] calculated the ligand-field parameters for octahedral Ni^{II} complexes with a bidentate ligand derived by condensation of 4-amino-3-mercapto-6-methyl-5-oxo-1,2,4-triazine with 3-(*p*-bromophenyl)-1-phenyl-1*H*-pyrazolecarboxaldehyde. For these complexes, the Racah *B* and *Dq* parameters were in the 720–760 cm^{-1} and 970–1060 cm^{-1}regions, respectively.

The same parameters calculated for nickel(II) complexes with Schiff base ligands derived from 4-aminoantipyrine are in the regions of $v = 610–830$ and 1110–1210 cm^{-1}, respectively.[29] Kurzak[30] discussed ligand-field parameters for six-coordinate nickel(II) complexes of the type $[Ni(py)_4L_2]$ (py = pyridine; L =

Table 4. Assignments, transition energies, and ligand-field parameters [cm^{-1}] for the [Ni(salpn)] complex in nonpolar solvents; symmetry D_{4h}, ground term $^1A_{1g}[D, E_g]$.

Assignment	MBz		DX		$CHCl_3$	
$^3E_g[F, T_{2g}]$	15160		15050		15400	
$^3A_{2g}[F, T_{1g}]$	15550		15690		15680	
$^3B_{1g}[F, A_{2g}]$	16410		16520		16480	
$^1A_{2g}[G, T_{1g}]$	17960		17990		17840	
$^1E_g[G, T_{1g}]$	19420		19410		19440	
$^1B_{1g}[D, E_g]$	20630		20640		20770	
$^1A_{1g}[G, E_g]$			36320		37340	
^1E_g [D, T_{2g}]			38150		37860	
$^1B_{2g}[G, T_{2g}]$			39050		38930	
$^1B_{1g}[G, E_g]$			40460		39330	
$^1B_{2g}[D, T_{2g}]$			40800		41010	
$^1E_g[G, T_{2g}]$			42070		42460	
$^1A_{1g}[S, A_{1g}]$			42520		42520	
RMS	100		200		200	
Dq_{xy}	1890	(20)	1880	(10)	1900	(10)
Ds	−3550	(50)	−3520	(20)	−3490	(10)
Dt	−1700	(20)	−1680	(10)	−1740	(10)
Ds/Dt	2.1		2.1		2.0	
B	270	(30)	250	(20)	240	(20)
C	1170	(90)	1140	(60)	1160	(30)
C/B	4.3		4.6		4.8	
e_σ	11360	(70)	11240	(50)	11320	(20)
$e_{\pi\perp}$	3810	(80)	3740	(40)	3740	(20)
$e_{\pi\parallel}$	6540	(90)	6400	(80)	6580	(20)

Table 3. Assignments, transition energies, and ligand-field parameters [cm^{-1}] for the [Ni(salpn)] complex in polar solvents; symmetry D_{4h}, ground term $^1A_{1g}[D, E_g]$.

Assignment	AC		DMF		DMSO		MeCN		*i*PrOH		EtOH		MeOH	
$^3E_g[F, T_{2g}]$	15060		15000		14920		15130		14790		15440		15390	
$^3A_{2g}[F, T_{1g}]$	15680		15760		15780		15770		15710		15940		15880	
$^3B_{1g}[F, A_{2g}]$	16500		16560		16560		16510		16560		16720		16720	
$^1A_{2g}[G, T_{1g}]$	17960		17940		17950		17940		17940		18100		18100	
$^1E_g[G, T_{1g}]$	19400		19470		19460		19480		19430		19380		19550	
$^1B_{1g}[D, E_g]$	20770		20770		20790		20770		20820		20640		20910	
$^1A_{1g}[G, E_g]$			37110		36770		36720		36760		37740		36630	
^1E_g [D, T_{2g}]							38460		38610		38500		38520	
$^1B_{2g}[G, T_{2g}]$							38970		39130		39130		39080	
$^1B_{1g}[G, E_g]$							40640		40620		40230		40660	
$^1B_{2g}[D, T_{2g}]$							41180		41190		41330		41280	
$^1E_g[G, T_{2g}]$							42860		42720		42770		43100	
$^1A_{1g}[S, A_{1g}]$							43280		43260		43000		43720	
$^1A_{1g}[G,A_{1g}]$							49020				48650		49830	
RMS	110		160		160		110		180		160		190	
Dq_{xy}	1880	(20)	1900	(10)	1890	(10)	1890	(10)	1900	(10)	1930	(10)	1890	(10)
Ds	−3590	(60)	−3560	(60)	−3590	(60)	−3590	(10)	−3580	(20)	−3500	(10)	−3650	(20)
Dt	−1710	(20)	−1740	(20)	−1730	(20)	−1710	(10)	−1720	(10)	−1760	(10)	−1730	(10)
Ds/Dt	2.1		2.0		2.1		2.1		2.1		2.0		2.1	
B	300	(40)	270	(30)	300	(30)	290	(10)	280	(10)	250	(10)	310	(20)
C	1090	(100)	1190	(80)	1110	(70)	1130	(30)	1190	(30)	1150	(10)	1120	(60)
C/B	3.7		4.4		3.7		3.9		4.3		4.5		3.7	
e_σ	11470	(70)	11460	(120)	11510	(80)	11450	(20)	11460	(20)	11400	(30)	11620	(10)
$e_{\pi\perp}$	3900	(60)	3840	(90)	3910	(50)	3860	(10)	3850	(20)	3740	(30)	3990	(20)
$e_{\pi\parallel}$	6700	(70)	6690	(130)	6770	(90)	6610	(30)	6640	(30)	6630	(60)	6830	(10)

 © 2018 The Authors. Published by Wiley-VCH Verlag GmbH & Co. KGaA, Weinheim

NCS^-, Cl^-, Br^-, I^-), and the Racah *B* and *C* parameters calculated for this complexes were higher than 860 and 3600 cm^{-1}, respectively.

For all of the studied solutions of [Ni(salpn)], the *Dq* parameter values are very similar and are equal to about 1900 cm^{-1} (Tables 3 and 4). The *C* parameter changes in the range of 1090 to 1200 cm^{-1}. Insignificant changes are observed for the *B* parameter with values in the range of 250 to 310 cm^{-1} (Tables 3 and 4). This suggests that the Racah parameter values are independent of the solvents used. The collected data indicate that for four-coordinate, square-planar nickel(II) complexes, the Racah parameter values are lower than those for six-coordinate complexes of nickel(II), but the *Dq* parameters are significantly greater than those typical of six-coordinate complexes.

la Cour et al.[31] presented results from the AOM for four-coordinate ketoimine Schiff base complexes in $CHCl_3$ solution. Their calculations were based only on two spin-allowed d–d transitions, that is, $^1A_{1g} \rightarrow {}^1A_{2g}$ and $^1A_{1g} \rightarrow {}^1B_{1g}$. Our calculations do not confirm these results, probably because configuration interactions were not included and because a very limited number of transitions were taken into account. The ligand-bonding abilities are characterized by an anisotropic π interaction, that is, the $e_{\pi\parallel}$ and $e_{\pi\perp}$ parameters were considered. [Ni(salpn)] is characterized by high e_σ and e_π values, and consequently, the donor atoms have very strong σ- and π-bonding abilities.[32] In all of the studied solvents, the σ interactions were stronger than the π and $\pi_\perp$ interactions are were almost two times weaker than the $\pi_\parallel$ interactions.

The AOM parameters were compared with some solvent parameters. No linear correlations were found. Nevertheless, it can be observed that for solvents of high and intermediate polarity, that is, MeCN, AC, EtOH, MeOH, *i*PrOH, DMSO, and DMF, the e_σ and $e_{\pi\parallel}$ values are lower than for solvents of low polarity, that is, DX, $CHCl_3$, and MBz. To determine the nature of ligand binding to the nickel(II) ion, the nepheloauxetic parameter was calculated. The value of this parameter in all solvents was found to be 0.22 to 0.28. These parameters indicate that the Ni–L bond is covalent in nature.

2.4. Solvatochromism of the Complex

As mentioned above, the two bands at $\nu = 24\,500$ and 37 500 cm^{-1} in the electronic spectra of [Ni(salpn)] are assigned to MLCT transitions. Their intensities and absorption maxima in a variety of solvents are reported in Table 5. As known, most solvents show solvatochromism, that is, the absorption maxima change upon changing the various solvent parameters. Evaluation of solvatochromism from electronic spectra is based on expressing transition energies, which correspond to absorption bands, in terms of a correlation with parameters characterizing the solvents: dielectric constant (ε), donor number (DN), acceptor number (AN), the Kosower parameter (*Z*), the Dimroth–Reichard Kosower parameter [$E_T(30)$], and the Kamlet and Taft (α and β) parameters. In Figure 8, the $MLCT_{Ni\rightarrow O}$ absorption maximum is plotted against the Dimroth–Reichards $E_T(30)$ parameters. The equation of the line of best fit is $\nu_{max} = (21\,938.4 \pm 134.9) + (48.1 \pm 3.0)E_T(30)$ with a correlation coefficient $R^2 = 0.97$. The same effect is observed for the Kosower parameter (*Z*) and the acceptor number (AN): $\nu_{max} = (21\,507.3 \pm 267.3) + (36.6 \pm 3.8)Z$ with a correlation coefficient $R^2 = 0.92$ and $\nu_{max} = (23\,486.5 \pm 88.4) + (26.2 \pm 3.6)$AN with

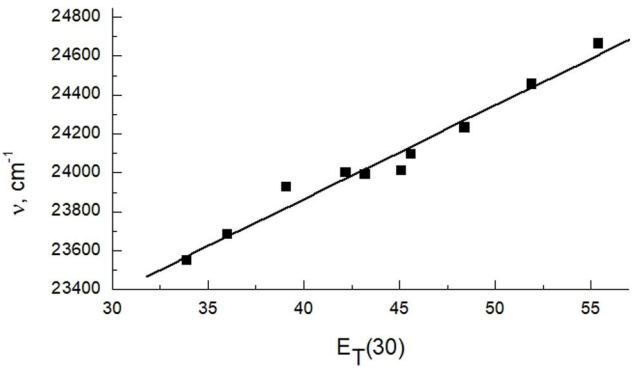

Figure 8. Correlation between the wavenumber of the $MLCT_{Ni\rightarrow O}$ band maximum and the Dimroth–Reichardt parameter [$E_T(30)$] for [Ni(salpn)] in the studied solvents.

Table 5. Solvent parameters [$E_T(30)$, *Z*, and AN] and intensities (ε_{max}) and positions (ν_{max}) of the CT resulting from the experimental curve and Gaussian analysis in the UV region in different solvents.

No.	Solvent	$E_T(30)$	*Z*	AN	$MLCT_{Ni\rightarrow O}$ exptl		calcd		$MLCT_{Ni\rightarrow N}$ exptl		calcd	
					ε_{max} [10^{-3} M^{-1} cm^{-1}]	ν_{max} [10^{-3} cm^{-1}]	ε_{max} [10^{-3} M^{-1} cm^{-1}]	ν_{max} [10^{-3} cm^{-1}]	ε_{max} [10^{-3} M^{-1} cm^{-1}]	ν_{max} [10^{-3} cm^{-1}]	ε_{max} [10^{-3} M^{-1} cm^{-1}]	ν_{max} [10^{-3} cm^{-1}]
1	MBz	33.9	54	6.8	6.09	23.56	4.27	23.55	–	–	–	–
2	DX	36.0	64.5	10.8	5.81	23.80	4.10	23.68	43.12	37.50	40.06	37.3
3	$CHCl_3$	39.1	63.2	23.1	6.47	23.90	3.94	23.93	48.97	37.84	34.97	37.2
4	AC	42.2	65.7	12.5	5.72	24.12	3.79	24.00	–	–	–	–
5	DMF	43.2	68.4	16.0	5.62	24.20	3.85	23.99	–	–	–	–
6	DMSO	45.1	70.2	19.3	5.30	24.36	3.55	24.01	38.23	37.54	32.78	37.2
7	MeCN	45.6	71.3	18.9	5.35	24.36	3.68	24.10	43.13	38.20	40.04	37.8
8	*i*PrOH	48.4	76.3	33.5	5.39	24.36	3.59	24.23	43.07	38.12	40.10	37.8
9	EtOH	51.9	79.6	37.1	5.23	24.68	3.25	24.46	44.35	38.38	40.22	37.9
10	MeOH	55.4	83.6	41.5	4.78	25.06	2.84	24.7	40.00	38.66	34.62	38.0

© 2018 The Authors. Published by Wiley-VCH Verlag GmbH & Co. KGaA, Weinheim

a correlation coefficient $R^2 = 0.87$, respectively. We found a strong linear correlation between the $MLCT_{Ni\rightarrow O}$ peak intensity and the Dimroth–Reichards parameters ($R^2 = 0.76$) with linear regression: $\varepsilon_{max} = (8278.9 \pm 561.1) - (61.3 \pm 12.6)E_T(30)$. Figure 9 presents the relationship between the $MLCT_{Ni\rightarrow O}$ absorption band intensities and the Dimroth–Reichards $E_T(30)$ parameter

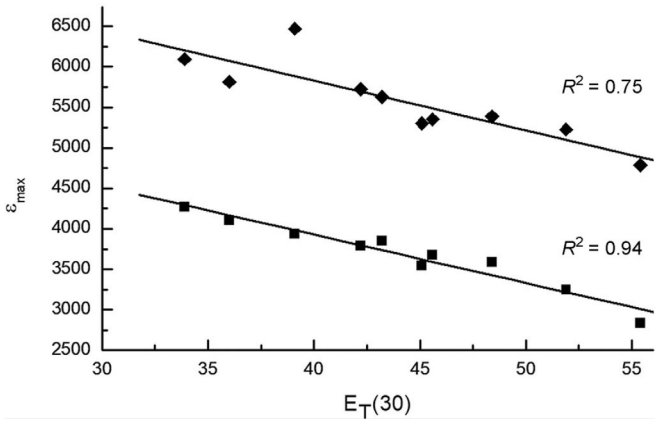

Figure 9. Correlation between the $MLCT_{Ni\rightarrow O}$ band intensities and the Dimroth–Reichardt parameter [$E_T(30)$] for [Ni(salpn)] in the studied solvents: ◆, experimental data (observed); ■, Gaussian analysis results.

for the experimental (◆) and Gaussian analysis (■) data. As can be seen, better results are obtained for the Gaussian analysis data ($R^2 = 0.94$ vs. $R^2 = 0.76$). In the experimental spectrum, we observe an overlapping effect of all transition types (MLCT, intramolecular, d–d). Gaussian analysis gives a possibility to consider only MLCT bands. The same effect is observed for the Kosower parameter (Z) and the acceptor number (AN) with regression lines of $\varepsilon_{max} = (6843.3 \pm 400.9) - (45.3 \pm 5.7)Z$ ($R^2 = 0.89$) and $\varepsilon_{max} = (4375.9 \pm 140.4) - (31.5 \pm 5.7)$AN ($R^2 = 0.80$), respectively. We also compared the positions and intensities of the $MLCT_{Ni\rightarrow N}$ absorption bands with the same solvent parameters. However, no correlations were found (Table 5).

2.5. Trichromaticity Colorimetry of Complexes

Trichromaticity colorimetry was used to determine the color of [Ni(salpn)]. In the electronic spectra (UV/Vis), changes in the positions of the bands as well as their intensities were observed upon changing the physicochemical properties of the solvents. All nickel(II) complex solutions under study are yellowish–green in color, and their electronic absorption spectra display two maxima at about $v = 16\,000$ (d–d transition) and 24 500 cm^{-1} in the region of $v = 12\,800$ to 26 300 cm^{-1}, which is a range often used to identify compounds by their color. Table 6 summarizes the calculation results of the chromaticity coordinates obtained from the absorption spectra of [Ni(salpn)] for all studied solutions. In the case of the reflectance spectra (solid sample), Kubelka–Munk theory[33] was applied for preliminary data transformation (R_F coefficient).

The colors of the solutions are herein reported in the CIE and CIELAB color spaces. These chromaticity parameters characterize the solutions unambiguously and allow color changes to be monitored. The L*, a*, and b* color space is uniform and recommended by CIE for color description. The L* parameter defines the psychometric lightness and corresponds to black (L* = 0) and white (L* = 100). The a* and b* parameters are psychometric chromaticness. Positive values of a* correspond to red, whereas negative values correspond to green. Positive b* values correspond to yellow, whereas negative values correspond to blue. The position of the color points on the CIELAB plane for the studied complex is presented in Figure 10. The colors of the [Ni(salpn)] solutions are represented by points on the chromaticity, positioned on the field of green–yellow hues.

Changes in the color properties of the [Ni(salen)] solutions were compared with some previously published solvent parameters.[34] The hue angle (h_{ab}), which is defined in Equation (1), was selected for comparison purposes, because it is very sensitive to changes in the intensities and positions of the absorption bands. For the studied Ni^{II} complex, linear correlations between the hue angle and the acceptor number were found for all of the solvents except AC. The data for all the studied solvents can be correlated as: $h_{ab} = (106.3 \pm 0.4) + (0.07 \pm 0.01)$AN with a correlation coefficient $R^2 = 0.90$.

Table 6. Chromaticity coordinates (CIE, CIELAB, and CIELUV spaces), hue angle (h_{ab}), and colors of [Ni(salpn)] in different solvents ($c \approx 1.0 \times 10^{-3}$ M, l = 0.2 cm) and the solid state.

Solvent	X	Y	x	y	z	L^*	a^*	b^*	c^*	h_{ab} [°]	u^*	v^*	Color[a]
MBz	79.0	91.5	0.38	0.44	0.19	96.6	−15.2	50.9	53.1	106.6	4.2	69.9	yellow green
DX	79.9	91.4	0.37	0.42	0.21	96.6	−13.5	44.9	46.8	106.7	4.3	63.0	yellow green
$CHCl_3$	81.1	92.7	0.36	0.41	0.22	97.1	−13.2	40.9	42.9	107.8	3.1	58.4	yellow green
AC	82.0	93.5	0.36	0.40	0.24	97.4	−11.4	36.1	38.1	109.9	3.5	52.4	yellow green
DMF	82.6	93.0	0.36	0.40	0.25	97.2	−11.1	33.8	35.6	108.1	2.9	49.6	yellow green
DMSO	83.2	93.4	0.35	0.40	0.25	97.4	−10.4	31.8	33.4	108.1	2.9	46.8	yellow green
MeCN	83.0	92.4	0.35	0.39	0.26	97.0	−9.1	28.9	30.3	107.6	3.3	42.8	yellow green
*i*PrOH	83.3	93.4	0.35	0.39	0.26	97.4	−10.3	30.0	31.7	108.9	2.2	44.6	yellow green
EtOH	83.3	92.8	0.35	0.39	0.27	97.2	−9.2	27.8	29.3	108.3	2.7	41.4	yellow green
MeOH	86.4	95.0	0.34	0.37	0.29	98.0	−7.2	19.8	21.1	109.8	1.4	30.5	yellow green
solid (R_F)	19.6	19.9	0.37	0.38	0.26	51.7	3.55	16.9	17.2	78.1	14.0	20.7	red yellow

[a] Color observed for solutions in 25 mL flasks.

© 2018 The Authors. Published by Wiley-VCH Verlag GmbH & Co. KGaA, Weinheim

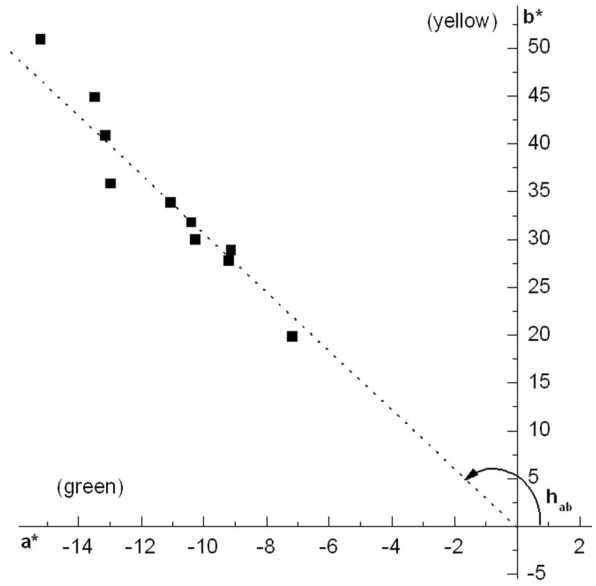

Figure 10. The CIELAB plane. The color points correspond to [Ni(salpn)] in all of the studied solvents.

$$h_{ab} = \text{arc tg}\left(\frac{b^*}{a^*}\right) \quad (1)$$

Thus, the calculated values of the color parameters of the [Ni(salpn)] complex enable the general spectroscopic changes observed in the absorption spectra to be combined with the properties of the solvents.

3. Conclusions

In summary, the nickel(II) complex with a tetradentate Schiff base ligand obtained by condensation of 1,3-propanediamine with salicylaldehyde (H_2salpn) was synthesized and characterized by various techniques, including elemental analysis, molar conductivities, IR spectroscopy, ultraviolet spectroscopy, and visible spectroscopy. The combined results of the spectrophotometric and conductance measurements confirmed that the solvent molecules were not coordinated to the metal ion in all of the studied solvents. The electronic spectra confirmed the square-planar geometry of the studied complex in solution. This indicated that, due to the presence of the strong-field tetradentate NOON ligand, no unpaired electrons were present in the Ni^{II} complexes. The results showed that the positions and intensities of the metal-to-ligand charge-transfer $(MLCT)_{Ni\rightarrow O}$ absorption bands clearly and significantly depended on the character of the solvent, whereas the positions and intensities of the $MLCT_{Ni\rightarrow N}$ bands did not depend on any solvent parameters. The values of the crystal field model and angular overlap model were almost the same in all of the systems studied and were independent of the solvent used. The calculated chromaticity coordinates indicated that the nickel complex is red-yellow in the solid state and yellow-green in all solutions.

Metal complexes with Schiff bases could become compounds with potentially very large practical applications, provided that we know their spectral properties very well. The results obtained in this paper are very informative and should be used to develop optoelectronic devices or in biological applications.

Experimental Section

Materials

All chemicals were of reagent grade and were used without further purification: salicylaldehyde (Honeywell Fluka), 1,3-diaminopropane (Sigma–Aldrich), and nickel(II) acetate tetrahydrate (POCH S.A.). All solvents were of spectroscopy grade; methanol, ethanol, chloroform, and acetone were purified, dried, and distilled before use.[35] The Schiff base ligand and nickel(II) complex were synthesized by the methods described below.

Synthesis

1,3-Bis(salicylideneimino)propane: The Schiff base ligand was prepared by a standard method.[15] Thus, a solution of 1,3-diaminopropane (4 mL) in EtOH (30 mL) was added to a solution of salicylaldehyde (10 mL) dissolved in hot ethanol (30 mL) (Scheme 2). The resulting mixture was then heated at reflux for approximately 1 h.

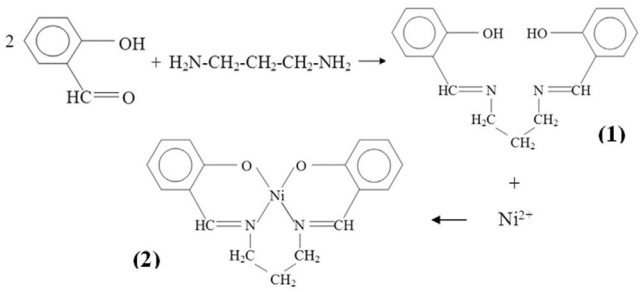

Scheme 2. Chemical synthesis of 1,3-bis(salicylideneimino)propane (**1**) and nickel(II) complex **2**.

After cooling, the yellow precipitate was filtered off, washed with ethanol, and dried in air at room temperature for several hours. Yield: 72%, m.p. 92–93 °C (94–96 °C from Ref. [15]); IR (KBr): $\tilde{\nu}$ = 3408 (O–H), 3052 (ArC–H), 2925 (C–H), 1636 (C=N), 1611 (C=C), 1447 (C=C), 1211 cm^{-1} (C–O); elemental analysis calcd (%) for $C_{17}H_{18}N_2O_2$ (282.34): C 72.32, H 6.43, N 9.92; found: C 72.20, H 6.53, N 9.97.

N′,*N*′-Propylenebis(salicylaldiminato)nickel(II): The nickel(II) complex was prepared by adding a solution of nickel(II) acetate tetrahydrate (1.5 g) in ethanol (15 mL) to the ligand (3.2 g), which was mixed with a few drops of triethylamine in hot ethanol (25 mL) (Scheme 2). The mixture was stirred at 50 °C for 2 h. After this time, the brown precipitate was filtered, washed with ethanol, and dried in air at room temperature. Yield: 64%; m.p. 304–305 °C (348 °C from Ref. [16]); IR (KBr): $\tilde{\nu}$ = 3060 (ArC–H), 2922 (C–H), 1611 (C=N), 1541 (C=C), 1476 (C=C), 1228 (C–O), 745 (Ni–N), 460 cm^{-1} (Ni–O); elemental analysis calcd (%) for $NiC_{17}H_{16}N_2O_2$ (339.01): C 60.23, H 4.76, N 8.26, Ni 17.31; found: C 60.03, H 4.73, N 8.29, Ni 16.30.

Physical Measurements

The nickel(II) content was estimated by the spectrophotometric method. Carbon, hydrogen, and nitrogen analyses were performed

© 2018 The Authors. Published by Wiley-VCH Verlag GmbH & Co. KGaA, Weinheim

by the Laboratory of Microanalysis and Automation of Analytical Methods (Polish Academy of Science, Łódź, Poland) using a Euro-Vector 3018 analyzer.

The solubility of the nickel(II) complex was investigated in 12 common solvents. It was insoluble in water (H_2O) and ethylene glycol (EG) but was easily soluble in common solvents such as dimethyl sulfoxide (DMSO), dimethylformamide (DMF), methanol (MeOH), ethanol (EtOH), 2-propanol (*i*PrOH), acetonitrile (MeCN), chloroform ($CHCl_3$), acetone (AC), dioxane (DX), and toluene (MBz). Solutions of [Ni(salpn)] were prepared by dissolving a weighed amount of the complex in a suitable solvent. The composition of the complex species in various solutions was confirmed by conductance measurements. The molar conductance was measured by using a microcomputer pH/conductivity meter CPC-551 (Elmetron, Poland) and a platinum dip electrode CD-2. The infrared spectra were obtained by using KBr with a Nicolet Magna IR 760 spectrophotometer. The near-IR spectrum (reflectance) of the solid complex was recorded with a CARY 5E (Varian) spectrophotometer. The electronic spectra of the ligand and nickel(II) complex solutions were recorded with a SPECORD M40 (Zeiss Jena) spectrophotometer about 15 min after dissolution. The measured spectra of the solutions were recorded digitally (20 cm^{-1} step) over the range of $\nu = 11\,000$ to 50 000 cm^{-1}at room temperature. The measurement conditions for the conductivity were the same as those for the electronic absorption spectra (i.e., $c \approx 1.0\times10^{-3}$ M). The UV/Vis spectra were resolved into Gaussian components and were used to study the solvatochromism and to calculate the chromaticity coordinates as well as the ligand-field (CFM/AOM) parameters.

The solvent parameters, the Kosower parameter (Z), the Dimroth–Reichardt parameter [$E_T(30)$], the Kamlet and Taft parameters (α, β, π^*), dielectric constant (ε), and Gutman's donor and acceptor numbers, were obtained from the literature.[36–41] Solvent effects could be the cause of both energy shifts of the absorption bands and changes in the solution color. The latter effect can be difficult to observe by the human eye. To characterize the color precisely, tristimulus colorimetry is usually used.[42–45] The chromaticity coordinates were calculated from the absorption spectra (in the region of $\lambda = 380$ to 780 nm) by the method described in the literature[43,46] for nonuniform (CIE) and two uniform (CIELAB and CIELUV) spaces by using the CIEC computer program.[47] This one is designed to calculate the color parameters for the solution, solid (reflectance), and simulated spectra. The CIE tristimulus values (X, Y, Z) expressed as integrals[43,46] were calculated as were the chromaticity coordinates (x, y, z) and two-space parameters: CIELAB (L^*, a^*, b^*) and CIELUV (L^*, u^*, v^*). The standard data[42,48] were built in the routine, that is, color matching functions taken every 5 (or 1) nm in the range of $\lambda = 380$ to 780 nm, as well as standard illuminance D_{65}. The absorption spectrum was transformed into the equivalent transmission spectrum.

Method of Calculations

Interpretation of the electronic spectra of the low-spin tetradentate Schiff base–nickel(II) complex was difficult for several reasons: 1) mutual overlapping of the low-symmetry components in the visible region (tetragonal splittings were not large enough in comparison with the spectral band widths); 2) overlapping more intensive CT [or intramolecular (IM)] bands in the near-UV region on d–d transitions in the visible region; because of this, the maxima of the d–d bands are not observed in the experimental curve. Most d–d transitions occur in the UV region and appear close to the intensive CT (or IM) bands. However, the former were taken into account in Gaussian analysis of their high intensities (ε equals about 1000 M^{-1} cm^{-1}).

Thus, for ligand-field interpretation of [Ni(salpn)], Gaussian analysis should be use for the visible and UV regions. All the band maxima reported here were determined from Gaussian analysis of the experimental spectral contours. Our calculations take into account all the transitions that are given by ligand-field theory. The absorption spectra of the nickel(II) complex and the ligand were fitted for Gaussian components by using the CFP (Curve Fitting Problem) computer program.[49] This program is based on the Slavič[50] numerical algorithm, which for the last few years has successfully been applied by us for the resolution of d–d (ligand-field) spectra.[30a,51,52] Our calculations of the CFM (crystal field model) and AOM (angular overlap model) parameters were performed for the Ni^{II} complex in different solutions by the LFP (Ligand Field Parameters) program[53] that uses two minimization techniques: the Powell method (nongradient) and the Davidon–Fletcher–Powell method (gradient estimation). The AOM calculations were performed within the framework of the angular overlap simple model developed by Schäffer[54,55] and Jørgensen.[56] For the CFM calculations, the full energy matrices reported by Perumareddi[57] were adopted in the LFP program. For AOM calculations, the matrix elements of the excited states given by Hitchman[58] were used, and the one-electron orbital energies given by Hitchman[59] were adopted. For the four-coordinate nickel(II) complexes (low-spin, d^8 electronic configuration, and D_{4h} symmetry), the ground state is $^1A_{1g}$, and a total of 18 d–d transitions were predicted by the CFM (11 spin allowed and 7 spin forbidden). All calculations were performed on an IBM microcomputer.

Conflict of Interest

The authors declare no conflict of interest.

Keywords: chromaticity · ligand-field parameters · nickel · Schiff bases · solvatochromism

[1] P. Przybylski, A. Huczynski, K. Pyta, B. Brzezinski, F. Bartl, *Curr Org Chem.* **2009**, *13*, 124 – 148.
[2] S. Shukla, R. S. Srivastava, S. K. Shrivastava, A. Sodhi, P. Kumar, *Med. Chem. Res.* **2013**, *22*, 1604 – 1617.
[3] C. M. Da Silva, D. L. Da Silva, L. V. Modolo, R. B. Alves, M. A. De Resende, C. V. B. Martins, A. De Fatima, *J. Adv. Res.* **2011**, *2*, 1 – 8.
[4] M. Manjunatha, V. H. Naik, A. D. Kulkarni, S. A. Patil, *J. Coord. Chem.* **2011**, *64*, 4264 – 4275.
[5] K. S. Kumar, S. Ganguly, R. Veerasamy, E. De Clercq, *Eur. J. Med. Chem.* **2010**, *45*, 5474 – 5479.
[6] S. Samadhiya, A. Halve, *Orient. J. Chem.* **2001**, *17*, 119 – 122.
[7] M. Alias, H. Kassum, C. Shakir, *J. Assoc. Arab Univ. Basic Appl. Sci.* **2014**, *15*, 28 – 34.
[8] H. F. Abd El-Halim, M. M. Omar, G. G. Mohamed, M. A. El-Ela Sayed, *Eur. J. Chem.* **2011**, *2*, 178 – 188.
[9] D. N. Dhar, C. L. Taploo, *J. Sci. Ind. Res.* **1982**, *41*, 501 – 506.
[10] A. Iwan, H. Janeczek, B. Jarząbek, P. Rannou, *Materials* **2009**, *2*, 38 – 61.
[11] M. Asadi, H. Sepehrpour, K. Mohammadi, *J. Serb. Chem. Soc.* **2011**, *76*, 63 – 74.
[12] D. A. Atwood, M. J. Harvey, *Chem. Rev.* **2001**, *101*, 37 – 52.
[13] K. Kurzak, A. Gonciarz, I. Kuźniarska-Biernacka, *Polish J. Chem.* **2005**, *79*, 47 – 56.
[14] O. Rotthaus, F. Tomas, O. Jarjayes, C. Philouze, E. Saint-Aman, J. Pierre, *Chem. Eur. J.* **2006**, *12*, 6953 – 6962.
[15] K. H. Chjo, B. G. Jeong, J. H. Kim, S. Jeon, C. P. Rim, Y. K. Choi, *Bull. Korean Chem. Soc.* **1997**, *18*, 850 – 856.

 © 2018 The Authors. Published by Wiley-VCH Verlag GmbH & Co. KGaA, Weinheim

[16] B. G. Jeong, C. P. Rim, S. K. Kook, K. H. Chjo, Y. K. Choi, *Bull. Korean Chem. Soc.* **1996**, *17*, 173 – 179.
[17] S. Zolezzi, A. Decinti, E. Spodine, *Polyhedron* **1999**, *18*, 897 – 904.
[18] M. Kanthimathi, B. U. Nair, T. Ramasami, J. Jeyakanthan, D. Velmurugan, *Transit. Metal. Chem.* **2000**, *25*, 145 – 149.
[19] J. Csaszar, J. Balog, *Acta Chim. Hung.* **1975**, *87*, 331 – 341.
[20] B. Bosnich, *J. Am. Chem. Soc.* **1968**, *90*, 627 – 632.
[21] K. Kurzak, I. Kuźniarka-Biernacka, B. Kurzak, J. Jezierska, *J. Solution Chem.* **2001**, *30*, 709 – 731.
[22] M. G. B. Drew, R. N. Prasad, R. P. Sharma, *Acta Crystallogr. Sect. C* **1985**, *41*, 1755 – 1758.
[23] I. P. Ejidike, P. A. Ajibade, *Molecules* **2015**, *20*, 9788 – 9802.
[24] S. Chattopadhyay, M. S. Ray, S. Chaudhuri, G. Mukhopadhyay, G. Bocelli, A. Cantoni, A. Ghosh, *Inorg. Chim. Acta* **2006**, *359*, 1367 – 1371.
[25] S. Yamada, *Coord. Chem. Rev.* **1966**, *1*, 415 – 437.
[26] K. S. Siddiqi, S. A. A. Nami, L. Chebude, Y. Chebude, *J. Braz. Chem. Soc.* **2006**, *17*, 107 – 112.
[27] R. H. Holm, *J. Am. Chem. Soc.* **1960**, *82*, 5632 – 5636.
[28] K. Singh, R. Thakur, V. Kumar, *Beni-Seuf Univ. J. Appl. Sci.* **2016**, *5*, 21 – 30.
[29] S. Chandra, D. Jain, A. K. Sharma, P. Sharma, *Molecules* **2009**, *14*, 174 – 190.
[30] a) K. Kurzak, A. Bartecki, *Transition Met. Chem.* **1988**, *13*, 224 – 229; b) K. Kurzak, A. Kołkowicz, A. Bartecki, *Polyhedron* **1991**, *10*, 1759 – 1765; c) K. Kurzak, A. Kołkowicz, A. Bartecki, *Transition Met. Chem.* **1992**, *17*, 155 – 158.
[31] A. la Cour, M. Findeinsen, R. Hazell, L. Henning, C. E. Olsen, O. Simonsen, *J. Chem. Soc. Dalton Trans.* **1996**, 3437 – 3447.
[32] M. A. Hitchman, *J. Chem. Soc. Faraday Trans.* **1972**, 846 – 851.
[33] G. Kortum, *Reflectance Spectroscopy. Principles, Methods, Applications* Springer, Berlin, **1969**.
[34] T. Tłaczała, *Pol. J. Chem.* **1997**, *71*, 823 – 830.
[35] D. D. Perrin, W. L. F. Armarego, *Purification of Laboratory Chemicals, 3rd ed.*, Pergamon Press, Oxford, **1988**.
[36] V. Gutmann, *Coordination Chemistry in Non-aqueous Solutions*, Springer, Vienna, **1968**.
[37] V. Gutmann, *The Donor-Acceptor Approach to Molecular Interactions*, Plenum Press, New York, **1978**.
[38] W. Linert, V. Gutmann, *Coord. Chem. Rev.* **1992**, *117*, 159 – 183.
[39] W. Mizerski, M. K. Kalinowski, *Monatsh. Chem.* **1992**, *123*, 675 – 686.
[40] Y. Markus, *Chem. Soc. Rev.* **1993**, *22*, 409 – 416.
[41] Y. Markus, *The Properties of Solvents*, Wiley, Chichester, **1998**.
[42] R. W. Hunt, *Measuring Colour*, Ellis Horwood, Chichester, **1987**.
[43] a) A. Bartecki, *The Colour of Metal Compounds* (in Polish), University of Technology Press, Wrocław, **1993**; b) A. Bartecki, J. Burgess, *The Colour of Metal Compounds*, Gordon and Breach, Amsterdam, **2000**.
[44] A. Bartecki, T. Tłaczała, *Spectrosc. Lett.* **1990**, *23*, 727 – 739.
[45] T. Tłaczała, A. Bartecki, *Monatsh. Chem.* **1997**, *128*, 225 – 234.
[46] F. M. Billmeyer, Jr., M. Salzman, *Principles of Colour Technology*, Wiley, New York, **1981**.
[47] K. Kurzak, unpublished computer program.
[48] W. Felhorski, W. Stanioch, *Tristimulus Colorimetry*, WN-T, Warsaw, **1973**.
[49] a) A. Bartecki, K. Kurzak, J. Myrczek, J. Sołtowski, J. Stelmaszek, *Computer Aided Spectral Measurements of Transition Metal Complexes.*, Report No. 18/80, University of Technology, Wrocław, **1980**, 1 – 278, in Polish; b) K. Kurzak, *Ph.D. Thesis*, University of Technology, Wrocław, **1983**, in Polish; c) A. Bartecki, J. Sołtowski, K. Kurzak, *Comput. Enhanced Spectrosc.* **1983**, *1*, 31.
[50] I. A. Slavič, *Nucl. Instrum. Methods* **1976**, *134*, 285 – 289.
[51] K. Kurzak, *Spectrochim. Acta* **1991**, *47A*, 1041 – 1050.
[52] a) K. Kurzak, *Wiad. Chem.* **1991**, *45*, 425 – 437; b) K. Kurzak, *Polish J. Chem.* **2000**, *74*, 331 – 347; c) I. Kuźniarska-Biernacka, K. Kurzak, B. Kurzak, J. Jezierska, *J. Solution Chem.* **2003**, *32*, 719 – 741.
[53] K. Kurzak, *Comp. Chem.* **2000**, *24*, 519 – 526.
[54] C. E. Schäffer, *Struct. Bonding (Berlin)* **1968**, *5*, 68 – 95.
[55] C. E. Schäffer, *Struct. Bonding (Berlin)* **1973**, *14*, 69 – 110.
[56] C. K. Jørgensen, *Modern Aspects of Ligand Field Theory*, North-Holland, Amsterdam, **1970**.
[57] J. R. Perumareddi, *J. Phys. Chem.* **1972**, *76*, 3401 – 3411.
[58] M. A. Hitchman, *Inorg. Chem.* **1972**, *11*, 2387 – 2393.
[59] M. A. Hitchman, *Inorg. Chem.* **1974**, *13*, 2218 – 2223.

Received: May 30, 2018

 © 2018 The Authors. Published by Wiley-VCH Verlag GmbH & Co. KGaA, Weinheim